STUDY OF ISI DISTRIBUTION IN PRESENCE OF DIFFERENT SOURCES OF NOISE IN LIF MODEL

A Dissertation submitted to the
School of Computer & Systems Sciences,
Jawaharlal Nehru University, New Delhi
in partial fulfillment of the requirements for the award of the degree
of

MASTER OF TECHNOLOGY
IN
COMPUTER SCIENCE AND TECHNOLOGY

BY
SUDHEER KUMAR SHARMA

UNDER SUPERVISION OF
PROF. KARMESHU

SCHOOL OF COMPUTER AND SYSTEMS SCIENCES
JAWAHARLAL NEHRU UNIVERSITY
NEW DELHI-110067, INDIA
JULY 2008

जवाहरलाल नॅहरू विश्वविद्यालय

JAWAHARLAL NEHRU UNIVERSITY

School of Computer & Systems Sciences

NEW DELHI- 110067, INDIA

CERTIFICATE

This is to certify that the dissertation entitled "**STUDY OF ISI DISTRIBUTION IN PRESENCE OF DIFFERENT SOURCES OF NOISE IN LIF MODEL**" being submitted by Mr. **Sudheer Kumar Sharma** to the School of Computer and Systems Sciences, **Jawaharlal Nehru University**, New Delhi, in partial fulfillment of the requirements for the award of the degree of **Master of Technology** in **Computer Science and Technology**, is a record of bonafide work carried out by him under the supervision of Prof. Karmeshu.

This work has not been submitted in part or full to any university or institution for the award of any degree or diploma.

Prof. Karmeshu
(Supervisor)
SC&SS, JNU, New Delhi

8/8/08
Prof. Parimala.N
(Dean, SC&SS,)
JNU, New Delhi

जवाहरलाल नॅहरू विश्वविद्यालय

JAWAHARLAL NEHRU UNIVERSITY

School of Computer & Systems Sciences

NEW DELHI- 110067, INDIA

DECLARATION

This is to certify that the dissertation entitled "**STUDY OF ISI DISTRIBUTION IN PRESENCE OF DIFFERENT SOURCES OF NOISE IN LIF MODEL**" is being submitted to the School of Computer and Systems Sciences, Jawaharlal Nehru University, New Delhi, in partial fulfillment of the requirements for the award of the degree of **Master of Technology** in **Computer Science & Technology**, is a record of bonafide work carried out by me.

The matter embodied in the dissertation has not been submitted for the award of any other degree or diploma in any university or institute.

Sudheer Kumar Sharma
29-07-08

July 2008
JNU, New Delhi

Sudheer Kumar Sharma
M.Tech, Final Semester,
SC&SS, JNU, New Delhi.

Dedicated to

Maa

ACKNOWLEDGEMENT

I would like to express my sincerest gratitude to my supervisor, Prof. Karmeshu for his outstanding guidance and support during my research. Without his valuable thoughts, recommendation and patience, I would have never been able to complete this work.

I wish to thank all my fellow students in Performance Modeling Lab for their help and support. I gratefully acknowledge the unselfish help given to me by Sanjeev, Miss K.V.Kadambari, Abhinav Gupta, and Vineet Khandelwal who inspired me greatly through many interesting discussions, support and feedbacks.

I want to say special thank to my senior Arun Kumar, Ashish Chaudhari, who went through research along side with me, gave me numerous assists both in academic and daily life.

I am also thankful to Gaurav, Ashutosh, Puran, Nitin and many more friends here in Jawaharlal Nehru University for making this period unforgettable and precious for me.

Finally, I am most thankful to my parents for their unlimited love, care and encouragement. Over the years, they cheer for even a tiny progress I made and always have faith in me no matter how difficult life is. Now it is time to dedicate this work to you.

Sudheer Kumar Sharma

ABSTRACT

Brain is the most complex organ in living being. The complexity of brain has always overwhelmed researchers, psychologists, and scientists. They are trying to map its behavior right from its evolution but only little success has been marked up till today. On the similar lines, we have concentrated on the most basic unit of the brain. Spikes are generated whenever the potential of the membrane of neuron reaches threshold value. Applying the concepts of Information theory, Monte Carlo technique and Pearson system of frequency curves to the inter spike interval distribution led to some exciting facts.

TABLE OF CONTENTS

Dissertation Title	i
Certificate	ii
Declaration	iii
Dedication	iv
Acknowledgment	v
Abstract	vi
Table of Contents	vii
List of Figures	ix
List of Tables	x
List of Abbreviations	xi

CHAPTERS

1. INTRODUCTION	1
Electrical properties of a neuron	2
Action Potential and Spike Generation	4
Neuronal Coding and Firing Rate	4
Noise and Stochasticity in neuronal system	5
Organization of dissertation	8
2. MODELING SINGLE NEURON AND NEUROINFORMATICS	9
2.1 Integrate and fire model	9
2.2 Hodgkin-Huxley Model	11
2.2.1Gating Theory	12
2.3Fitzhung-Nagumo model	12
2.4 Neural Information Processing	13
2.4.1 Measure of Uncertainty: Entropy	13
2.4.2 Mutual Information	14
2.4.3 Measure of Directed Divergence	15
2.4.5 Entropy Measure for Continuous Variate	15
2.5 Information of Spiking Neuron	16

3. NON-LEAKY ISI DISTRIBUTION: ANALYSIS, MONTE CARLO APPROACH AND PEARSON CURVES 19
3.1 Non-leaky Integrate-fire Model 20
3.2 FPT: Monte Carlo Simulation 21
3.3 Pearson Frequency Curve 25
3.4 Approximation of FPT distribution and Pearson Curves 26

4. ISI DISTRIBUTION OF LIF MODEL WITH WHITE NOISE AND COLORED NOISE: MONTE CARLO STUDY 30
4.1 Stochastic LIF model with white noise 31
4.2 Approximating PDF of simulated FPT: Pearson Curve 35
4.3 Leaky-Integrate and Fire Model with Colored Noise 36
4.4 Approximating FPT distribution by Pearson Curve 39
4.5 Effect of ν on K L measure 41

5. CONCLUSION 43

List of Figures

Figure 1.1 Equivalent circuit of neuron. 3

Figure 2.1 Spike generation 10

Figure 3.1, Probability density function of inverse Gaussian function..... 21

Figure 3.2, Wiener increment process with respect to time..... 22

Figure 3.3, FPT: Monte-Carlo simulation of membrane potential..... 22

Figure 3.4, Histogram of the simulated ISI distribution..... 23

Figure 3.5, Probability density function of simulated and exact ISI..... 24

distribution.

Figure 3.6, Pearson plot obtained from the simulated data..... 29

Figure 4.1 Simulated runs of membrane potential..... 33

Figure 4.2, Histogram for simulated ISI distribution..... 34

Figure 4.3, Probability density function of simulated ISI distribution of... 34
leaky integrate and fire model

Figure 4.4, Pearson Type VI curve generated from simulated data..... 36

Figure 4.5a Histogram of ISI data of LIF model with color noise and v=10. 37

Figure 4.5b Histogram of ISI data of LIF model with color noise and v=50. 38

Figure 4.5c Histogram of ISI data of LIF model with color noise and v=100. 38

Figure 4.6, PDF of simulated ISI distribution of LIF model with colored 39

noise at different value of neu parameter

Figure 4.7, Type VI frequency distribution 41

Figure 4.8, Variation of K L-measure between ISI distributions with color noise and ISI distribution with white noise 42

List of Tables

Table 3.1 Types of frequency curves..... 24

Table 3.2 Data from histogram in fig 3.4..... 27

Table 4.1 Data from histogram in fig 4.2..... 35

Table 4.2: centre value of bins and frequency obtained from histogram for ν=100 40

List of Abbreviations

ISI	Inter Spike Interval
LIF	Leaky Integrate and Fire
O-U	Ornstein Uhlenbeck
H-H	Hodgkin-Huxley
IF-FHN	Integrate and Fire Fitzhung-Nagumo
FPT	First Passage Time
PDF	Probability Density Function
IF	Integrate and fire
SDE	Stochastic Differential Equation
CN	Colored Noise
WN	White Noise
IGD	Inverse Gaussian Distribution

Chapter-1

Introduction

Computational neuroscience is an approach to deal with the study of behavior of neurons. It provides an understanding of the mechanism for generation and processing of information. To this end, several models have been developed at different structural scales for gaining better insight into information processing mechanism. The development of models in neuroscience aims to capture various aspects. They range from a detailed description of biophysical models to a model of a single neuron based on the electrical properties of its membrane [1]. The main challenge in the field of computational neuroscience is to understand the process of information generation from sensory inputs. The most basic unit of brain is neuron. Normal human beings have approximately 10^{12} neurons. The nerve cells of nervous system are capable of carrying information through electrochemical processes, which involve flow of Sodium and Potassium ions. Computational modeling aims to help in determining functions of nervous system [2].

Neurons consist of a cell body, dendrites and an axon. Dendrite is responsible for bringing information to the neuron and axon for sending information to other neuron. This establishes communication between the neurons. A neuronal cell comprises 1.Dendrites, 2.Nucleus, 3.Axon, 4.Myelin sheath, 5.Schwann cell, 6.Axon Terminal, and 7.Node of Ranvier

Neurons are grouped in huge numbers in array of ions along with molecules. Many molecules have positive or negative charges. There is

preponderance of negative charge within a neuron. The cell membrane of the neuron is a lipid bilayer 3 to 4nm wide so as to be basically impervious to the majority of the charged molecules. This shielding characteristic causes the cell membrane to perform as a capacitor by straightening out the charges lying by the side of its internal and external surface [1].

The potential of the extracellular fluid outside a neuron is defined to be 0. When a neuron is inactive, the excess internal negative charge causes the potential inside the cell membrane to be negative. This potential is in equilibrium when the flow of ions into the cell matches with the out flow. The potential can change if the balance of ion flow is modified by the opening or closing of ion channels. Under normal conditions, neuronal membrane potential varies over a range from about -90 to +50 mV. The order of magnitude of these potentials can be estimated from basic physical properties [1, 2].

1.1 Electrical properties of a neuron

The electrical properties of neurons and the biophysical mechanism are well established which are responsible for neuronal activity. Accordingly, it is natural that for a large neuronal network, one would be confronted with an enormously large number of differential equations. Accordingly, attempts have made to look for simpler models which besides capturing salient features of neuronal dynamics, also are analytically tractable. The electrical properties of neurons are generally captured in terms of membrane potential, which changes when the flow of ions is modified, by opening and closing of ion channels [2].

The membrane potential of the nerve cell changes very rapidly. The ions provide a rich substrate for generating nonlinear operation. The membrane potential is a crucial variable, which govern the dynamics of neuronal operation. The difference between the potential of inner and outer membrane of the neuron is referred to as membrane potential $V_m(t)$, which is given by

$$V_{m(t)} = V_i - V_o(t) \tag{1}$$

where V_i is potential of inner surface and V_o is potential of outer surface.

The value of the resting potential varies between –30 mV to –90 mV; the resting potential is the potential difference at an equilibrium point at which the inward flow is equal to outward flow. The charge collected at the membrane is proportional to the capacitance of the membrane,

$$Q = C_m V_m \tag{2}$$

where C_m is the capacitance of the membrane. Denoting the neuronal current represented by Ic, we have

$$I_C = C\frac{dV_m}{dt} \tag{3}$$

This current is generated on account of change in potential between the surfaces. Actually, there is no movement of charge across the insulating membrane but there is a change of density of charge along the membrane surface. This causes variation in potential. Following Koch [1], the equivalent circuit is depicted in fig 1.

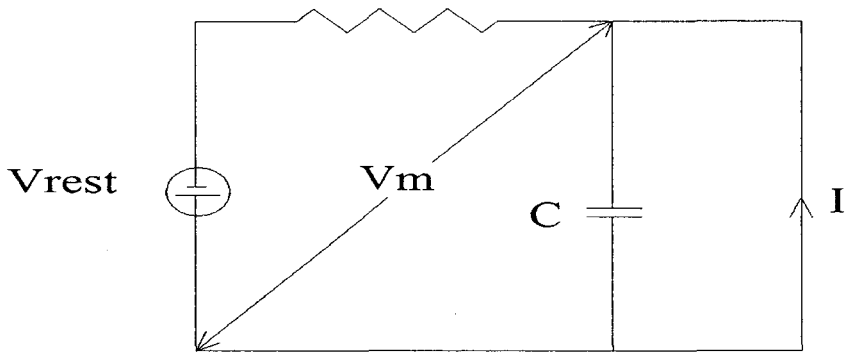

Figure 1.1, Equivalent circuit of neuron.(Adapted from [1])
Applying Kirchhoff's law, we get

$$RC\frac{dV_m}{dt} = -V_m + V_{rest} + RI \qquad (4)$$

where R is the membrane resistance, C is membrane capacitance, Vm is membrane potential and I is the current due to the flow of ions

1.2 Action Potential and Spike Generation

It is well established that with the increase of membrane potential above a threshold, the neuron generates action potential in the form of spike. As pointed out in [1], the action potential may have to 100 mV fluctuations and is dependent on the recent history. The action potential in the form of membrane potential fluctuation can traverse over large distances. Potential fluctuations, which correspond to subthreshold, do propagate only very small distance and get attenuated very fast [2]. A problem of interest is to obtain the relationship between stimulus and response. One of the difficulties is that several neurons respond to stimuli and one would like to determine the firing pattern of a single neuron.

1.3 Neuronal Coding and Firing Rate:

The problem of neuronal coding is not well understood. As noted by Gerstner and Kristler [3] that in a small part of brain, say cortex, thousand of spikes are produced every millisecond. The question is to characterize the code used by neurons to transmit information. The challenge is to understand the message, which can be inferred from the neuronal activity. One of the quantities, which can provide insight, is the mean firing rate. If $\{t_1, t_2, t_3...\}$ denote the times at which the neuron fires, then the spike sequence can mathematically represented as a sum of delta function (see Dayan and Abbott [2]).

$$\rho(t) = \sum_{i=1}^{n} \delta(t - t_i) \qquad (5)$$

Such that $0 \leq t_i \leq T$. The neuronal response in the form of spikes varies from trial to trial; one way to deal with such a situation is to take average

$$r(t) = \frac{n}{T} = \frac{1}{T}\int_0^T \rho(\tau)\, d\tau \qquad (6)$$

where r represents spike count rate.

When one averages over multiple trials, then average firing rate or spike-count rate becomes time dependent, i.e.

$$r(t) = \frac{1}{\Delta t}\int_t^{t+\Delta t} \langle \rho(\tau) \rangle d\tau, \qquad (7)$$

where $\langle \rho(\tau) \rangle$ denotes averaging over different trials and can be viewed as ensemble average. Using this formalism, it is possible to define spike-triggered average stimulus as

$$C(\tau) = \frac{1}{\langle n \rangle} \int_0^T r(t)s(t-\tau)\,dt \qquad (8)$$

Here <n> is the average number of spikes per trial. In a similar manner one can define the correlation function [2] of the firing rate and the stimulus as

$$Q_{rs}(\tau) = \frac{1}{T} \int_0^T r(t)s(t-\tau)dt \qquad (9)$$

The white noise stimulus is characterized by delta-correlated function, i.e.

$$Q_{ss}(\tau) = {\sigma_s}^2 \delta(\tau) \qquad (10)$$

1.4 Noise and Stochasticity in neuronal system

A fundamental question in neuroscience is concerned with the issue of transmission of information from stimuli to the central nervous system. The sequence of spikes signals information: It is now well established that noise and statistical fluctuations are present in all biological systems. The irregularity of spike could be on account of stochasticity and thus to get an estimate of spike rate, one would be required to pool responses from many neurons. In contrast to this viewpoint, it is suggested that variability results from coincidence of presynaptic events [4]. In both viewpoints, it can be argued that the randomness in ISI distribution is essential for information transfer through neuronal code.

The presence of stochasticity is essentially of biophysical origin emanating from irregular presynaptic spike trains, unreliable transmitter release and stochastic ion channel gating postsynaptic ion channel noise [5].

As noted by Robinson [5], low frequencies in noise spectrum play a significant role in changing the membrane potential. The noise is

generally exponentially correlated. Such type of noise can be generated from the Ornstein Uhlenbeck process with dynamics

$$\frac{dX}{dt} = -\frac{X}{\tau} + \sigma r(t) \tag{11}$$

where τ is the time constant ,σ is the magnitude of fluctuation and r(t) is a white noise process i.e.

$$E[r(t)] = 0 \tag{12}$$

$$E[r(t_1)r(t_2)] = \delta(t_2 - t_1) \tag{13}$$

In a more rigorous mathematical selling, the white-noise process can be associated with a Wiener process,

$$\{W(t), t \geq 0\}$$

Eq(11) can be written as

$$dX(t) = -\frac{X}{\tau}dt + \sigma dW(t) \tag{14}$$

Eq(12) represents a Ornstein-Uhlenbeck process which belongs to diffusion process. In contrast to noise source being modeled by Poisson process which has been gainfully employed to capture discontinuities in the form of sudden change in field potentials and brain recordings [6].

As observed by Tuckwell and Feng [6] that excitatory and inhibitory synaptic potential exhibit jumps. One of the earlier models due to Gerstein

and Mandelbrot [7], represent the difference of two Poisson processes corresponding to excitatory and inhibitory input given by

$$dX = a_E dN_E - a_I dN_I; \quad a_E, a_I \geq 0 \tag{15}$$

Mathematically, it is convenient to resort to diffusion approximation where one approximates eq (16) by a Stochastic Differential Equation

$$X = (\lambda_E a_E - \lambda_I a_I)dt + \sqrt{(\lambda_E a_E^2 + \lambda_I a_I^2)}dW(t) \tag{16}$$

This Stochastic Differential Equation is discussed in Tuckwell and Feng [6], It essentially represents Brownian motion with drift $(\lambda_E a_E - \lambda_I a_I)$ and fluctuations$(\lambda_E a_E^2 + \lambda_I a_I^2)$.

One can associate a Fokker-Planck equation with eq (14), viz.

$$\frac{\partial p(x,t)}{\partial t} = -(\lambda_E a_E - \lambda_I a_I)\frac{\partial p}{\partial x} + \frac{1}{2}(\lambda_E a_E^2 + \lambda_I a_I^2)\frac{\partial^2 p}{\partial x^2} \tag{17}$$

This equation gives the probabilistic description of the variable x(t) at any time point. With appropriate boundary conditions, the solution of eq (18) is a Gaussian process. The first passage time solution of eq (17) is the well known inverse Gaussian distribution viz.

$$f(t) = \frac{(V_t - V_0)}{\sqrt{2\pi\sigma^2 t^3}} \exp\left(\frac{-(V_t - V_0 - \mu t)^2}{2\sigma^2 t}\right) \tag{18}$$

where

$$\mu = \lambda_E a_E - \lambda_I a_I \tag{19}$$

and

$$\sigma^2 = \lambda_E a_E^2 + \lambda_I a_I^2 \qquad (20)$$

with $V_{th} > V_0$;

1.5. Organization of Dissertation

The dissertation consists of five chapters. The first chapter gives an overview of the field of computational neuroscience and some of the mathematical tools which are needed. The second chapter deals with the fields of modeling of single neuronal dynamics and neuroinformatics. The well known models viz. LIF, H-H are discussed from the point of neuronal coding, the basic quantitative formula based on information theory is briefly discussed. The third chapter deals with the Monte Carlo simulation procedure for non-leaky integrate-fire model. The closeness of first passage time distribution obtained by Monte Carlo simulation is compared with the exact inverse-gaussian distribution. This is done by employing K L measure. A new method is proposed based on Pearson frequency curve method to identify the functional form of probability distribution of FPT for ISI. The next chapter discusses the effect of colored noise on leaky integrate-fire model. Extensive simulations are carried to contrast ISI distribution with colored noise from that of white noise. Again Pearson type VI frequency curve is found to characterize FPT distributions. In terms of K L measure, FPT distributions for ISI with colored noise are found to converge in the limiting case to that of white noise. The last chapter contain conclusion.

Chapter-2

Modeling Single Neuron and Neuroinformatics

The aim of understanding stochastic dynamics of a single neuron is to shed light on brain architecture and functions like perception, cognition and information processing. Accordingly, the area of information processing by single neuron in different part of nervous system has been an active area of research (Moss and Gielen,[12]). Recording responses simultaneously from a large number of neurons is difficult; it becomes convenient to draw inference from single neuron firings. We shall closely follow the description of single neuron as given by [6]. Though the dynamics of a single neuron is controlled by several variables, one of the important variables turn out to be membrane potential.

The spike timings when action potential reaches the threshold are recorded in the form of series of time events $\{t_1, t_2, t_3 \ldots\}$, where t_i denotes the arrival time of i^{th} spike. Most of the information, which is conveyed by the nerve cell, is also conveyed by time series. The issue of coding of information in the form of spikes has led to the development of the field of neuroinformatics. In this chapter, we briefly outline the models of single neuron, spike generation and analysis of spiking train [1, 2].
The well-known model, called as integrated and fire model, has been extensively studied to provide understanding of the mechanism for spike generation.

2.1 Integrate and Fire Model

It is well established that as the membrane potential V(t) reaches a threshold value V_{th} at the T^*, the action potential occurs resulting in spike generation. After this the potential is reset to resting potential V_{rest} such that $V(T^{*+})=V_{rest}$.

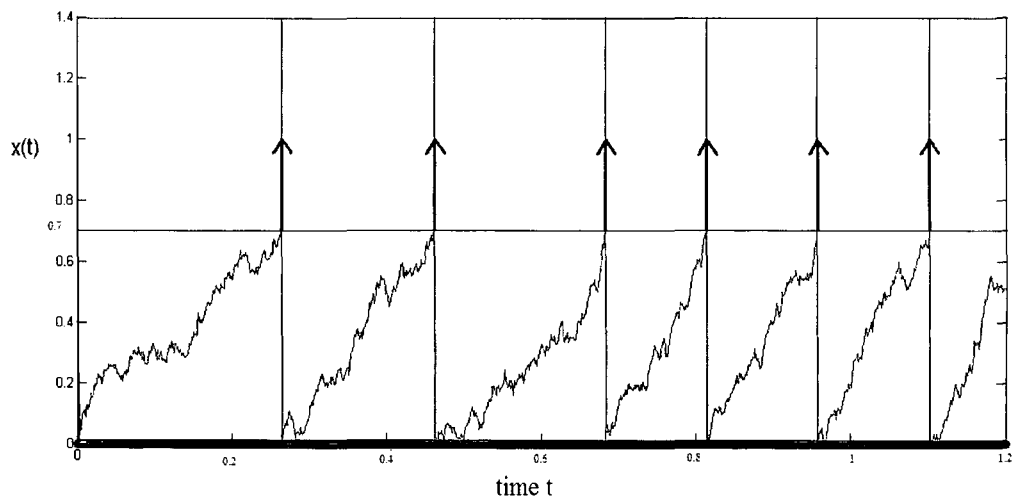

Figure 2.1 Spike generation with $V_{th}=0.7$

This process explains the mechanism of spike generation. One may refer to figure 2.1 depicting the random variation in the membrane potential V(t) resulting in generation of spike when $V(t)=V_{th}=0.7$. A refractory period is the time interval after which the process of another spike generation is initiated [2].

The differential equation when $V<V_{th}$, is given by

$$\frac{dV}{dt} = \frac{-(V(t)-V_{rest})}{\tau} + I(t) \qquad (1)$$

where I(t) is the input current and Vrest is the resting potential and τ is the membrane time constant. Thus if the refractory period is T_{ref} then $V(t+T_{ref}) = V_{rest}$.

Eq (1) is a linear differential equation which can be explicitly solved to yield time-dependent potential. It easily seen that membrane potential varies exponentially with the time constant τ

There are other well-known models which along with integrate and fire model are, classified as point model:

1. Hodgkin-Huxley model.
2. Fitzhugh-Nagumo model.

2.2 Hodgkin-Huxley Model

This model provides the basic biophysical mechanism for the action potential and elucidates the nonlinear properties of neuronal membrane. Hodgkin-Huxley derived the set of four nonlinear differential equations as a mechanism for action potential regeneration [12],

$$C_m \frac{dV}{dt} = G_{leak}(V_{leak} - V) + G_{Na} m^3 h (V_{Na} - V) + G_K n^4 (V_K - V) \quad (2)$$

$$\tau_m \frac{dm}{dt} = m_\infty(V) - m \quad (3)$$

$$\tau_h \frac{dh}{dt} = h_\infty(V) - h \quad (4)$$

$$\tau_n \frac{dn}{dt} = n_\infty(V) - n \qquad (5)$$

The membrane capacitance is denoted by C_m, the parameters G_{leak}, G_{Na} and G_K represent the conductance of the leak current, sodium current and potassium current. The parameters n, m are the activation variable of the potassium, sodium current, h is inactivation variable of sodium current (see Meunier and Segev [13]).

On account of faster activation process, the voltage increases from resting potential V_{rest} to certain value V_0 and starts decreasing because of slower inactivation. The potential evolves on account of the flow of different currents into the membrane. When the potential rises from V_{rest} to V_0, initially the sodium current increases rapidly due to activation constant m and after that it decreases slowly due to inactivation constant h.

2.2.1 Gating Theory

Hodgkin-Huxley [2] gives the detailed description in terms of membrane properties, which provide mechanism for generation of action potential. The state variable represents two states, namely the open and closed states. Accordingly, the channel switches randomly from one state to another and vice versa. The activation variable n can be viewed as probability of switching of channel being open at a certain time. The differential equation for the activation process becomes.

$$\frac{dn}{dt} = a_n(V)(1 - n) - b_n(V)n, \qquad (6)$$

where rate function $a_n(V)$ and $b_n(V)$ are defined as

$$\tau_n(V) = \frac{1}{a_n(V)+b_n(V)} \qquad (7)$$

$$n_{\infty}(V) = \frac{a_n(V)}{a_n(V)+b_n(V)} \qquad (8)$$

The rate function a_n and b_n are the transition rates from closed to open state and vice versa [2].

2.3 Fitzhung-Nagumo Model

This model is a reduced description of Hodgkin-Huxley model and captures the basic features of spike generation. In terms of membrane potential V and recovery variable W, Tuckwell and Feng [6], describe the dynamics as

$$\frac{dV}{dt} = k[-V(V-\alpha)(V-1) - W] + I \qquad (9)$$

$$\frac{dW}{dt} = [V - cW] \qquad (10)$$

Here k, b, α, c is constant. If a threshold potential is investigated then the model is referred to IF-FHN (integrate and fire Fitzhung-Nagumo model)

2.4 Neural Information Processing

Gabbiani and Koch [8], have brought out the necessity of a stochastic framework in neuronal coding. If the spikes are regularly spaced, the amount of information received is zero. This aspect has necessitated that the spiking pattern should involve randomness. Naturally one interested in finding the relationship between variability and neural coding. The quantitative measure of variability and uncertainty is provided by information theory [11]. We briefly describe the salient feature of quantifying uncertainty based on information theory.

2.4.1 Measure of Uncertainty: Entropy

Shannon [9, 10] developed a measure uncertainty in terms of entropy. For a probability distribution $P=\{p_1,p_2,p_3,\ldots p_n\}$, the entropy is defined as

$$H_n(P) = -\sum_{i=1}^{n} p_i log_2 p_i \quad \text{bit} \qquad (11)$$

We take 0log0=0. It is easy to see that $0 \leq H_n(P) \leq log_2 n$ the entropy is 0 while it is maximum when $P= \{\frac{1}{n},\frac{1}{n},\frac{1}{n}\ldots \frac{1}{n}\}$. The maximum values of entropy correspond to the case when all outcomes have equal probability i.e. uniformly distributed.

Shannon entropy function has several properties which are listed the in book of Kapur and Kesavan [9]

$P=\{p_1,p_2,p_3,\ldots p_n\}$, and $Q=\{q_1,q_2,q_3,\ldots q_m\}$, are two independent probability distribution associated with random variables X and Y i.e

$P(X=x_i)=p_i, \quad i=1,2\ldots n.$
$P(Y=y_j)=q_j, \quad j=1,2\ldots m.$
$P(X=x_i, Y=y_j)=r_{ij}=p_i.q_j, \quad i=1,2\ldots n, \; j=1,2\ldots m$

It can be seen that the joint entropy equals the sum of entropies of random variables X and Y, we have

$$H_{mn}(P * Q) = -\sum_i \sum_j r_{ij} \log r_{ij} = H_n(P) + H_m(Q) \qquad (12)$$

2.4.2 Mutual Information

Consider a stochastic system with input X and Y. The entropy H(X) denotes the uncertainty of the input. On observing the output Y, the uncertainty of X is reduced and is given by H(X|Y). The conditional entropy H(X|Y) represents the remaining of uncertainty of X once Y is observed. Thus one can define a measure of mutual information [10, 11] i.e. dependence between X and Y as

$$I(X, Y)=H(X)-H(X|Y) \qquad (13)$$

Eq(13) can be rewritten as

$$I(X,Y) = \sum_i \sum_j p(x_i, y_j)\log\left[\frac{p(x_i,y_j)}{p(x_i)q(y_j)}\right] \qquad (14)$$

It can easily seen that $I(X,Y)\geq 0$. When X and Y are independent random variables, then

$$I(X, Y) =0$$

The mutual information measure I(X, Y) is symmetric, i.e.

$$I(X, Y) =I(Y, X)$$

The reason as to why mutual information is useful in information processing is due to the fact that one can characterize the input –output relations in the context of spiking neuron

2.4.3 Measure of Directed Divergence

Kullback and Leibler proposed a measure of directed divergence D(P||Q) between two probability distributions[11]: This measure provides a measure of distance of probability distribution P from that Q and is defined as

$$D(P||Q) = \sum_{i=1}^{n} p_i log \frac{p_i}{q_i} \qquad (15)$$

It may be noted that this measure is not symmetric i.e. D(P||Q)≠D(P||Q). When two distributions become identical, then D(P||Q)=0.

2.4.5 Entropy Measure For Continuous Variate

The entropy for continuous variate X having pdf f(x) is defined as

$$H(X) = -\int f(x) \ln f(x)\, dx \qquad (16)$$

It must be pointed out that this form is not limiting form of discrete variate (for details see Karmeshu [10]).

2.5 Information of Spiking Neuron

It is known that spikes carry information and the temporal sequence of spikes provide a big reservoir for transmitting information. A fundamental question: which of the two features is employed by brain? Big reservoir or variability in spike times?

The variability in spike times with evolving stimuli can be captured by entropy per unit time (see Strong et al [14]). We define $\Delta\tau$ as the bin size, and T as the window length, then the entropy is given by

$$S(T, \Delta t) = -\sum p_i \log p_i \qquad (17)$$

where p_i is the normalized count of the i^{th} word. Here we consider an example from Strong et.al [14], where $\Delta\tau$=3 ms, T=100 ms then S≈ 17.8 bits

Strong et.al [14] in their paper provides an approach to quantify neuronal information in bits.

Chapter-3

Non-leaky ISI Distribution: Analysis, Monte Carlo Approach and Pearson Curves

The membrane potential of the neuron increases due to the electrochemical processes inside the neuron [1, 2]. The time epoch the membrane potential reaches a certain threshold value for the first time known as first passage time (FPT). The spike is generated and after that the membrane potential decays to a value known as resting potential. Many researchers have advanced theoretical arguments regarding behavior of FPT. The first passage time is random in nature [13]. The difference between time epochs of two consecutive spikes is known as Inter Spike Interval generally known as ISI interval. The collections of ISI intervals yield probability distribution. Varieties of mathematical models are proposed to study ISI distribution. Mathematically, the first passage time can be defined as

$$T = \inf\{t \geq 0 |\ V(t) > S,\ V(0) < S\} \qquad (1)$$

It can be seen that T is a random variable, which depends on the stochastic dynamics of the membrane potential. From the realization of the random variable T, one can calculate inter-spike intervals. As observed by Maio, Lansky and Rodriguez [15] the analysis of ISI distribution is done in terms of moments when the form of probability distribution is very difficult to obtain.

3.1 Non-Leaky Integrate-Fire Model

The non-leaky integrate-fire is described by a stochastic differential equation

$$\tau dV = \mu dt + \sigma dW(t) \qquad (2)$$

where τ is a membrane constant given by τ=RC, and σ is the magnitude of fluctuations and dW(t) is known as wiener process increment.

Interestingly, this equation is similar to the one proposed by Gerstein and Mandelbrot [7], which reads as

$$dV = (\lambda_E a_E - \lambda_I a_I)dt + \sqrt{(\lambda_E a_E^2 + \lambda_I a_I^2)}dW(t) \qquad (3)$$

where the symbol have been defined in chapter 1 (see section 1.4).
Here

$$\mu = \lambda_E a_E - \lambda_I a_I \quad \text{and } \sigma^2 = \lambda_E a_E^2 + \lambda_I a_I^2 \qquad (4)$$

For $\mu>0$, the FPT is given by inverse-gaussian distribution.

$$f(t) = \frac{S}{\sqrt{2\pi\sigma^2 t^3}} \exp\left(\frac{-(S-\mu t)}{2\sigma^2 t}\right), \; t \geq 0 \qquad (5)$$

The plot of the PDF is shown in figure 3.1

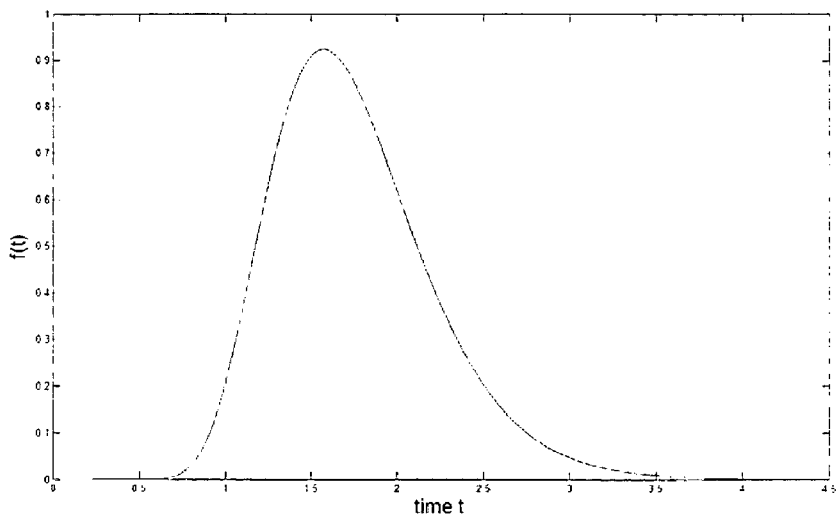

Figure 3.1, Probability density function of inverse Gaussian function
The value of σ^2=0.02, S=0.7;

3.2 FPT: Monte Carlo Simulation

The SDE (2) can be discretized by using Euler method. Discretizing the time interval (0, T) into equal sub-intervals of size h= $\frac{T}{N}$, such that τ_n=nh (i.e. τ_0=0, τ_1=h, τ_2=2h,...).

Following Gardiner [16], the Monte Carlo simulation of SDE is based on Euler method. Introducing the Wiener increment dW(h) = W(t+h)-W(t)≅ $\sqrt{h}Z$, Z~N(0,1), SDE (2) can be discretized as

$$V((n+1)h) = V(nh) + \mu h + \sigma\sqrt{h}Z_n \qquad (6)$$

where $Z_0, Z_1, \ldots$ are independent and identically distributed standard normal variates. Lansky, Sanda and He [19], has suggested a similar approach based on Euler discretization earlier.

We present a sample path corresponding to Wiener-increment in Fig 3.2

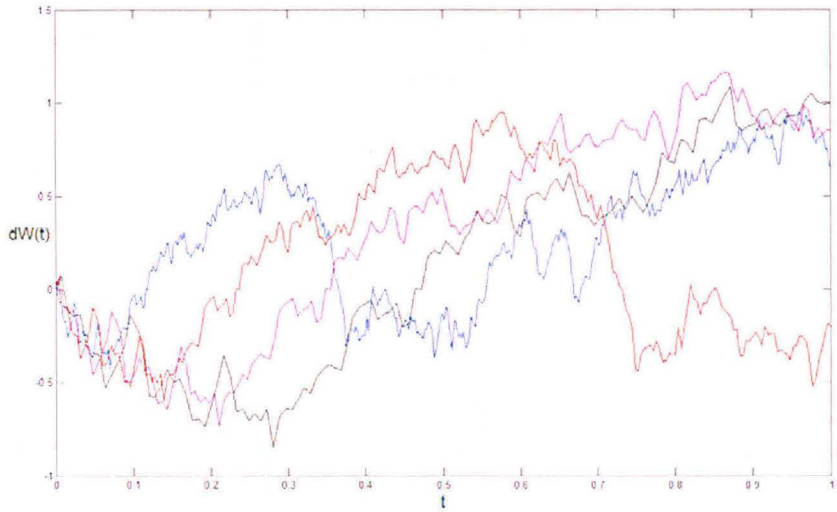

Figure 3.2, Wiener increment process with respect to time.

Simulate of SDE (2). The realization of first passage time is given in figure 3.3

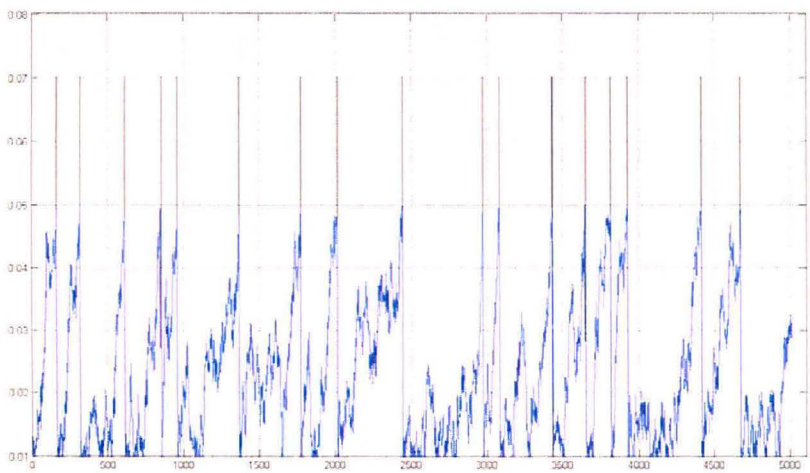

Figure 3.3, FPT: Monte-Carlo simulation of membrane potential reaching threshold for the first time V_{th}=0.05, V_{rest} is 0.01, h=0.01, σ=0.1414.

We have carried out about $O(10^5)$ simulations for inter-spike intervals. The total number of steps corresponding time increments is $O(10^6)$. Noting that sampling error in Monte Carlo is $O(n^{-1/2})$, we find that sampling errors are considerably reduced.

From the collection of ISI, we have constructed histogram as shown in figure 3.4

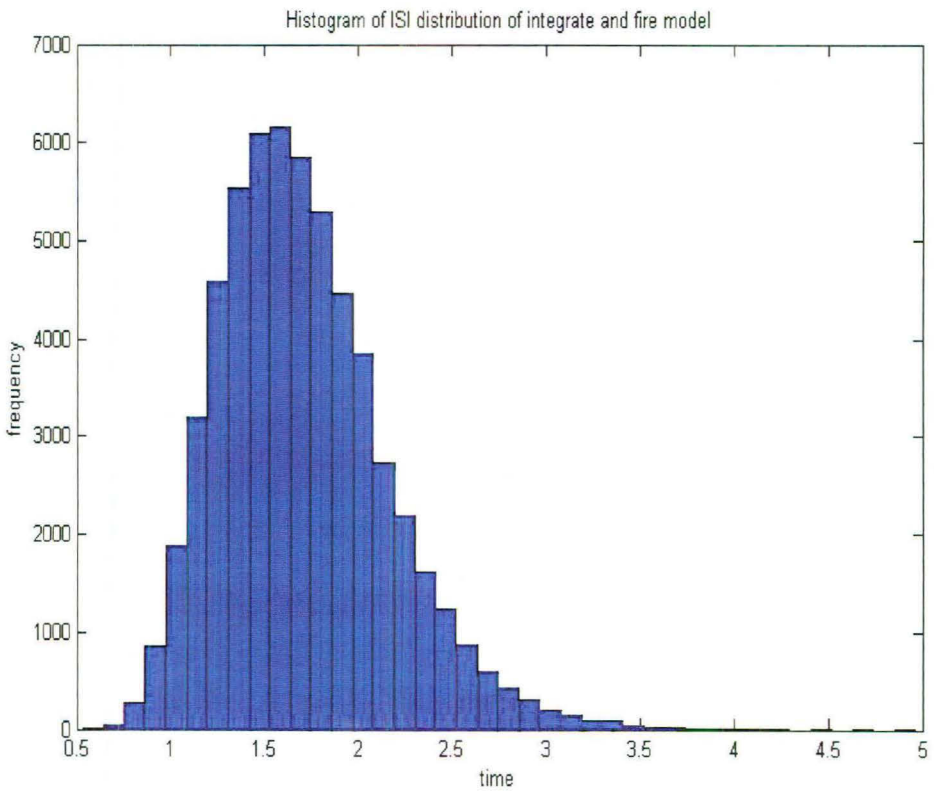

Figure 3.4, Histogram of the simulated ISI distribution.

In order to check the efficacy of Monte Carlo simulations and exact FPT, we plot the probability densities in figure 3.5

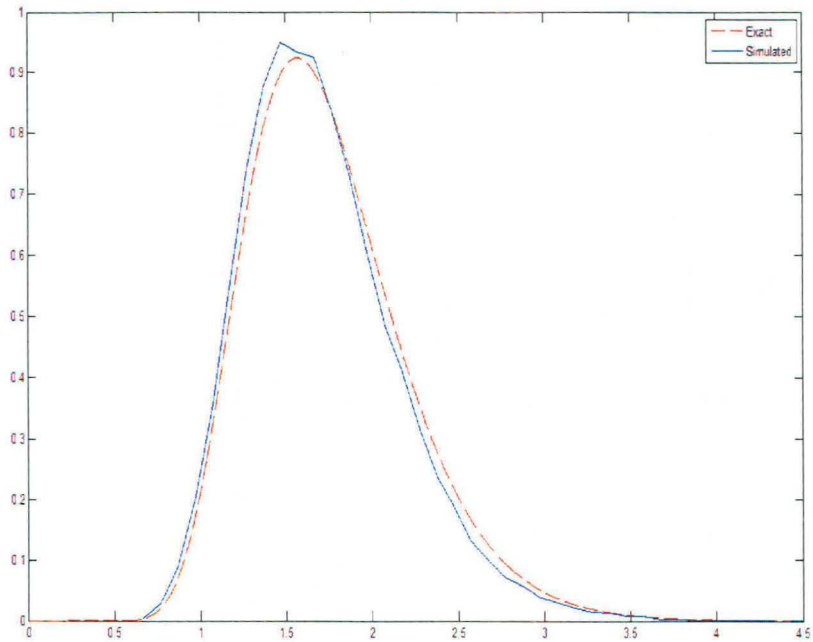

Figure 3.5, Probability density function of simulated and exact ISI distribution.

For investigating, goodness of fit of Monte Carlo FPT with that of a exact inverse-gaussian distribution, we compute K.L measure of distance between simulated distribution from that of exact distribution.

Denoting by $P=\{p_1, p_2, p_3, \ldots p_n\}$ the simulated distribution and $Q=\{q_1, q_2, q_3, \ldots q_m\}$ the exact distribution, the K L measure is defined as

$$D(P||Q) \cong \sum_{i=1} \left(p_i * log \frac{p_i}{q_i} \right) \qquad (7)$$

In our case D(P||Q) turns out to be 0.0541.

3.3 Pearson Frequency Curve:

The FPT for non-leaky IF model can be described by an exact distribution. In general it is not possible to have exact expression. To this end, we explore the possibility of identifying the frequency curve based on Pearson system as discussed in the book by Elderton and Johnson [17]. For the sake of completeness, we briefly outline the procedure.

Pearson argued that unimodal curves can be obtained from the solution of differential equation

$$\frac{1}{y}\frac{dy}{dx} = \frac{a+x}{b_0+b_1x+b_2x^2} \qquad (8)$$

where a, b_0, b_1 and b_2 are constant parameters. He outlined a procedure for obtaining the parameters by the method of moments. Multiplying Eq(8) by x^n and integrating, we get

$$\int x^n(b_0 + b_1x + b_2x^2)\frac{dy}{dx} = \int y(x + a)x^n dx \qquad (9)$$

Assuming that y vanishes at the end points, Eq(9) yield

$$-nb_0\mu_{n-1}' - (n + 1)b_1\mu_n' - (n + 2)b_2\mu_{n+1}' - \ldots = \mu_{n+1}' + a\mu_n' \qquad (10)$$

where

$$\mu_n' = \int yx^n dx \qquad (11)$$

Eq(10) can be used to provide moment estimates for the unknown parameters. Pearson noted that there exist 12 forms depending in parameter κ, β_1 and β_2. Elderton and Johnson [17] have classified the frequency curves as given in table 3.1

Table 3.1

Criterion	Type
$\kappa = -\infty$	III
$-\infty < \kappa < 0$	I
$\kappa = 0, \beta_2 = 3\ \beta_1 = 0$	Normal curve,
$\kappa = 0, \beta_2 < 3$ and $\beta_1 = 0$	II
$\kappa = 0$, $\beta_1 = 0$ and $\beta_2 > 3$	VII
$0 < \kappa < 1$	IV
$\kappa = 1$	V
$\kappa > 1$	VI
$\kappa < 0, \lambda = 0$, and $5\beta_2 - 6\beta_1 - 9 < 0$	VIII
$\kappa < 0, \lambda = 0$, and $5\beta_2 - 6\beta_1 - 9 > 0$	IX
$\beta_2 = 9, \beta_1 = 4$	X
$\kappa > 1, \lambda = 0$, $2\beta_2 - 3\beta_1 - 6 > 0$	XI
$5\beta_2 - 6\beta_1 - 9 > 0$	XII

3.4. Approximation of FPT distribution and Pearson Curves

From the simulated ISI distribution, we have to calculate values of κ, $\beta 1$ and β_2 to identify the type of Pearson curve [21],

Pearson defined

$$\kappa = \frac{\beta_1(\beta_2+3)^2}{4(4\beta_2-3\beta_1)(2\beta_2-3\beta_1-6)} \qquad (12)$$

$$\beta_1 = \frac{{\mu_3}^2}{{\mu_2}^3}, \quad \beta_2 = \frac{\mu_4}{{\mu_2}^2} \qquad (13)$$

For calculating κ, $\beta 1$ and β_2 we refer to table 3.2.

Table 3.2

central value of bins	frequency	First Sum	Second Sum	Third Sum	Fourth Sum
0.6868	49	58589	505659	2769185	12154566
0.8205	384	58540	447070	2263526	9385381
0.9542	1479	58156	388530	1816456	7121855
1.0878	2985	56677	330374	1427926	5305399
1.2215	4825	53692	273697	1097552	3877473
1.3552	7082	48867	220005	823855	2779921
1.4888	7212	41785	171138	603850	1956066
1.6225	7219	34573	129353	432712	1352216
1.7562	6978	27354	94780	303359	919504
1.8898	5445	20376	67426	208579	616145
2.0235	4430	14931	47050	141153	407566
2.1572	3207	10501	32119	94103	266413
2.2908	2317	7294	21618	61984	172310
2.4245	1768	4977	14324	40366	110326
2.5582	1038	3209	9347	26042	69960
2.6918	731	2171	6138	16695	43918
2.8255	511	1440	3967	10557	27223
2.9592	322	929	2527	6590	16666
3.0928	218	607	1598	4063	10076
3.2265	143	389	991	2465	6013
3.3602	98	246	602	1474	3548
3.4938	66	148	356	872	2074
3.6275	35	82	208	516	1202
3.762	17	47	126	308	686
3.8948	10	30	79	182	378
4.0285	5	20	49	103	196
4.1622	9	15	29	54	93
4.2958	1	6	14	25	39
4.4295	2	5	8	11	14
4.5632	3	3	3	3	3

$$S_2 = \frac{sum(first\ sum)}{sum(frequency)}$$
$$S_3 = \frac{sum(second\ sum)}{sum(frequency)}$$
$$S_4 = \frac{sum(third\ sum)}{sum(frequency)}$$
$$S_5 = \frac{sum(fourth\ sum)}{sum(frequency)}$$

$$d = S_2$$

$$\vartheta_2 = 2 * S_3 - d(1+d)$$

$$\vartheta_3 = 6 * S_4 - 3 * \vartheta_2(1+d) - d(1+d)(2+d)$$

$$\vartheta_4 = 24 * S_5 - 2\vartheta_3(2(1+d)+1) - \vartheta_2(6(1+d)(d+2)-1) - d(1+d)(d+2)(d+3)$$

And moments are calculated as

$$\mu_2 = \vartheta_2 - \left(\frac{1}{12}\right),\ \mu_3 = \vartheta_3 \text{ and } \mu_4 = \vartheta_4 - \left(\frac{1}{2}\right)\vartheta_2 + \left(\frac{7}{240}\right)$$

The importance of Pearson method lies in the fact that it has enabled us to identify the functional form of the FPT distribution.

From the foregoing computation we find κ=1.810.

As κ>1, we conclude that the simulated corresponds to Pearson type VI curve

Type VI Curve:

The functional form of FPT distribution f(t) belongs to type VI with density function

$$y \equiv f(t) = y_0(t-a)^{q_2}t^{-q_1} \qquad (14)$$

where y0 is the normalization constant

$$y_0 = \frac{Na^{(q_1-q_2-1)}\Gamma(q_1)}{\Gamma(q_1-q_2-1)\Gamma(q_2+1)} \qquad (15)$$

Where q1 and q2 are given by

$$\frac{r-2}{2} \pm \frac{r(r+2)}{2}\sqrt{\frac{\beta_1}{\beta_1(r+2)^2+16(r+1)}} \qquad (16)$$

and r is given by

$$r = \frac{6(\beta_2-\beta_1-1)}{6+3\beta_1-2\beta_2} \qquad (17)$$

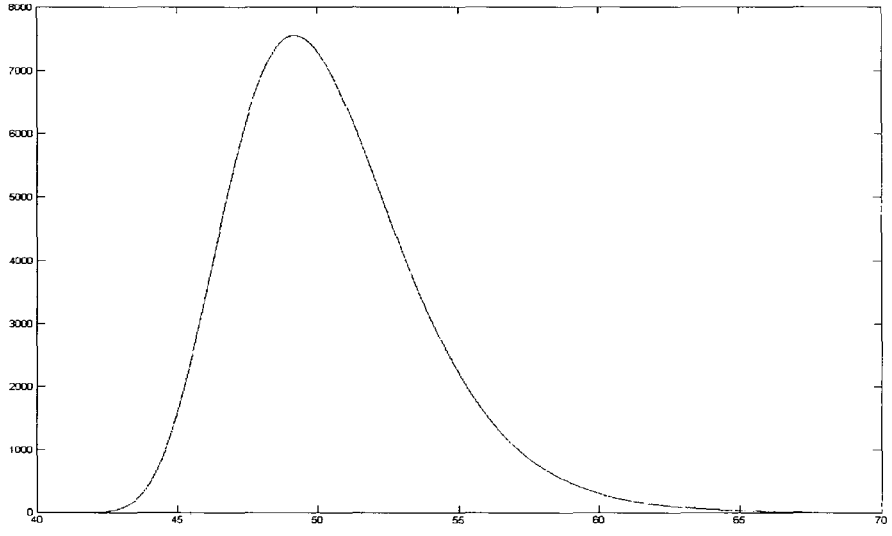

Figure 3.6, Pearson plot obtained from the simulated data

Chapter-4

ISI distribution of LIF Model with White noise and Colored noise: Monte Carlo Study

One of the widely used models is based on Leaky Integrate and Fire, which can be recovered from detailed biophysical models (Koch 1998; Dayan and Abbot, 2001 [1, 2]). The justification for LIF is that with properly selected threshold, it can produce spike in a fairly large number of cases which describes 90% of spikes correctly [3]. Various researchers have established the fact that LIF model though simple, describes a realistic neuronal model. In this model, the variable of interest is membrane potential. This model can be described in terms of a circuit with a generator, a resistor and a capacitor in parallel. The model neuron generates a spike when the potential reaches a threshold and thereafter the value of the potential is reset to its initial value [8].

It is well established that the spikes pattern suggest the existence of inherent random noise in the neuronal activity. The random noise can be present either in the input signal or in target neuron (Maio, Lansky and Rodriguez 2004). Adding a stochastic term in the differential equation governing the dynamics of membrane potential captures the randomness in the neuronal activity; accordingly, the mathematical description is provided by stochastic differential equation (SDE). These models are inherently nonlinear. Accordingly, one has to simulate these models to gain an understanding of the behavior of the system. One of the major tasks of the model development is to capture interspike interval (ISI) distribution. This will require detailed analysis of the system's output for various parameters of the model. It may be pointed out that the

parameters like conductance, capacitance, and input current are assumed to remain fixed. We now describe briefly the well-known LIF model. Leaky integrate and fire model is based on Nernst equation. The membrane potential V_m can either go up or go down depending on the flow of charge out of cell or flow of charge into the cell .[1]

Representing by V_L the Leak potential, one finds the membrane potential goes down when $V_m > V_L$ and the membrane potential goes up when $>V_L$ [1]. The differential equation for Vm is

$$C_m = \frac{dV_m}{dt} = \frac{G_L(V(t)-V_0)}{R} + I(t), \quad V(0) = V_0 , \qquad (1)$$

where G_L and C_m denote conductance and capacitance respectively and I(t) denotes the applied current. Equation (1) can be rewritten as,

$$\frac{dV_m}{dt} = \frac{-V(t)}{\tau} + \mu(t), \quad V(0) = 0 \qquad (2)$$

Here τ=RC is a time constant governing the decay of the voltage back to its initial value and $\mu(t) = I(t)/C$. In LIF model neuronal firing takes place whenever the depolarization V(t) reaches the threshold value S, thereafter depolarization V(t) is immediately reset to initial value, the time elapsed between two consecutive crossings of the threshold (spikes) defines an interspike interval(ISI).

4.1 Stochastic LIF Model with White Noise

The introduction of stochasticity into the LIF model is done by adding noise into equation (2). The model is described by a stochastic differential equation

$$\frac{dX(t)}{dt} = \frac{-V(t)}{\tau} + \mu(t) + \sigma\xi(t), \quad X(0) = 0 \qquad (3)$$

where ξ (t) represent a δ- correlated Gaussian noise with zero mean and strength σ.

Here μ (t) is any deterministic signal. The solution of Eq(3) as a first passage time provides an understanding of ISI distribution. Mathematically we can write

$$T=\inf\{t\geq 0|X(0)=0\} \qquad (4)$$

The initial condition is X(0)=0. In general it is not possible to explicitly compute the first passage time distribution. Only in special cases, expressions of the first passage time are available.

SDE and Simulation

In general setting it is not possible to have an analytical expression for FPT which will provide ISI distribution. Therefore, one is required to simulate SDE. One of the simplest numerical schemes is based on Euler scheme developed for ordinary differential equation. In this scheme the SDE(3) in terms of Weiner increment becomes

$$\frac{dV(t)}{dt} = \left[\frac{-V(t)}{\tau} + \mu(t)\right]dt + \sigma dW(t), \quad V(0) = 0 \qquad (5)$$

Using Euler discretization (as discussed in chapter 3),

$$V((n+1)h) - V(nh) = \frac{-V(nh)h}{\tau} + \mu h + \sigma\sqrt{h}Z_n \qquad (6)$$

Here h represents the time-step Z are independent and normally distributed random variables such that Z ~N(0,1), where Z0, Z1, ... are independent, identically distributed standard normal variates.

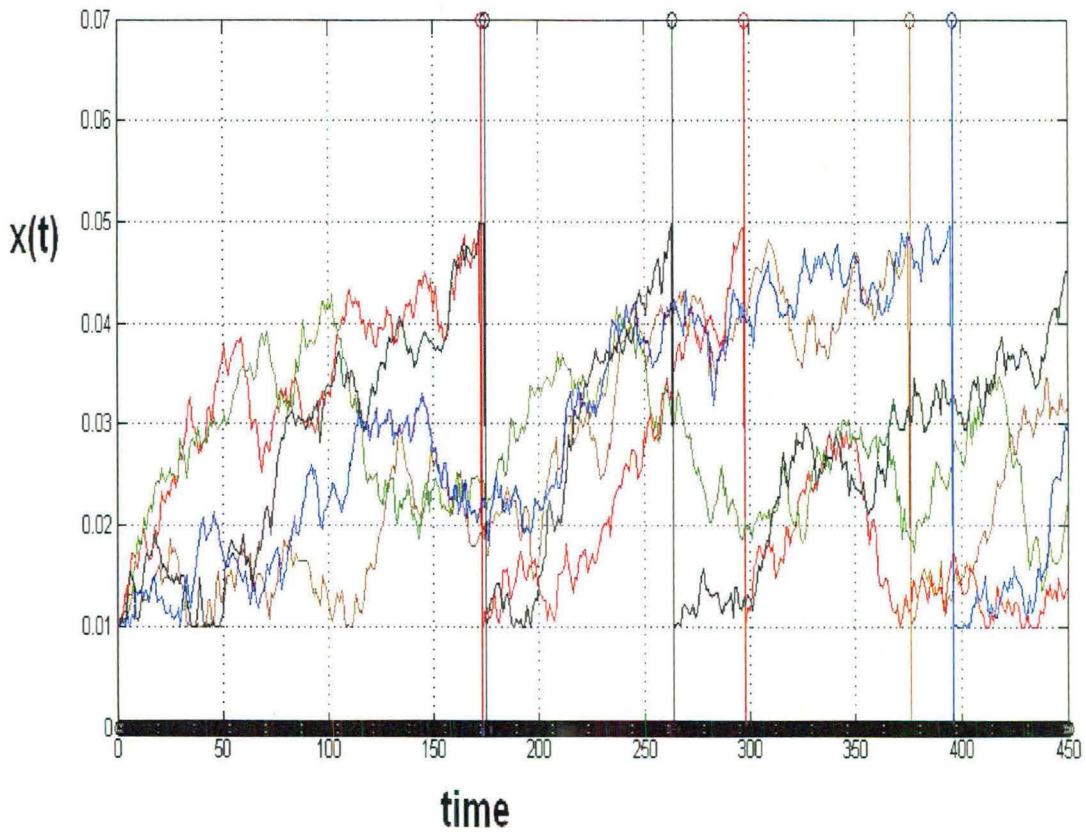

Figure 4.1 Simulated runs of membrane potential, Resting potential 0.01, Threshold value 0.05,

We generate standard normally distributed random numbers and update the value of potential at each time epoch as described by eq(6). In fig 1, we describe five simulations and spike generation whenever the potential reaches the threshold potential.

From the simulation runs we collect data corresponding Inter-spike intervals. These ISI's enable us to construct histogram and the

corresponding probability density function of FPT. The histogram is given in fig 4.2 and the corresponding PDF is shown fig 4.3.

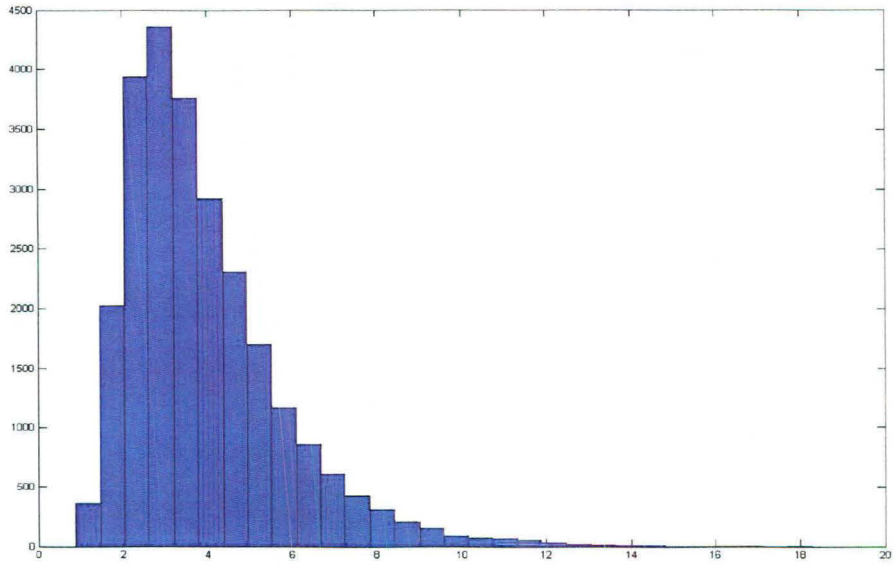

Figure 4.2, Histogram for simulated ISI distribution

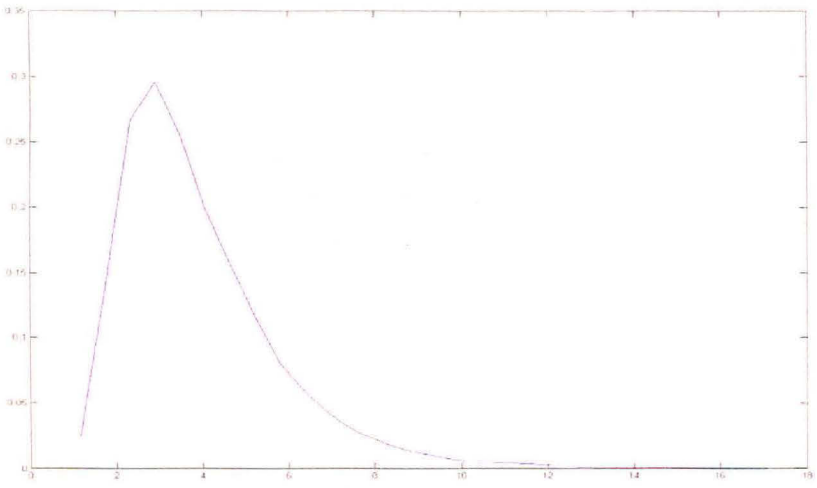

Figure 4.3, Probability density function of simulated ISI distribution of leaky integrate and fire model

4.2 Approximating PDF of Simulated FPT: Pearson Curve

As outlined in chapter 3, we attempt to identify the Pearson curve for the data sets shown in Table 1.

Table 4.1 Data from histogram in fig 4.2.

central value of bins	frequency	First sum	Second Sum	Third Sum	Fourth Sum
1.1698	363	25467	146804	628559	2400315
1.7495	2025	25104	121337	481755	1771756
2.3292	3935	23079	96233	360418	1290001
2.9088	4358	19144	73154	264185	929583
3.4885	3760	14786	54010	191031	665398
4.0682	2918	11026	39224	137021	474367
4.6478	2302	8108	28198	97797	337346
5.2275	1698	5806	20090	69599	239549
5.8072	1168	4108	14284	49509	169950
6.3868	859	2940	10176	35225	120441
6.9665	608	2081	7236	25049	85216
7.5462	420	1473	5155	17813	60167
8.1258	307	1053	3682	12658	42354
8.7055	209	746	2629	8976	29696
9.2852	153	537	1883	6347	20720
9.8648	93	384	1346	4464	14373
10.4445	77	291	962	3118	9909
11.0242	70	214	671	2156	6791
11.6038	49	144	457	1485	4635
12.1835	33	95	313	1028	3150
12.7632	18	62	218	715	2122
13.3428	13	44	156	497	1407
13.9225	6	31	112	341	910
14.5022	7	25	81	229	569
15.0818	5	18	56	148	340
15.6615	4	13	38	92	192
16.2412	2	9	25	54	100
16.8208	2	7	16	29	46
17.4005	1	5	9	13	17
17.9802	4	4	4	4	4

Carrying out similar analysis as done in chapter 3 we find κ=5.7637 which is >1. This indicates that the frequency curve is of Pearson type VI. The curve is plotted in fig 4

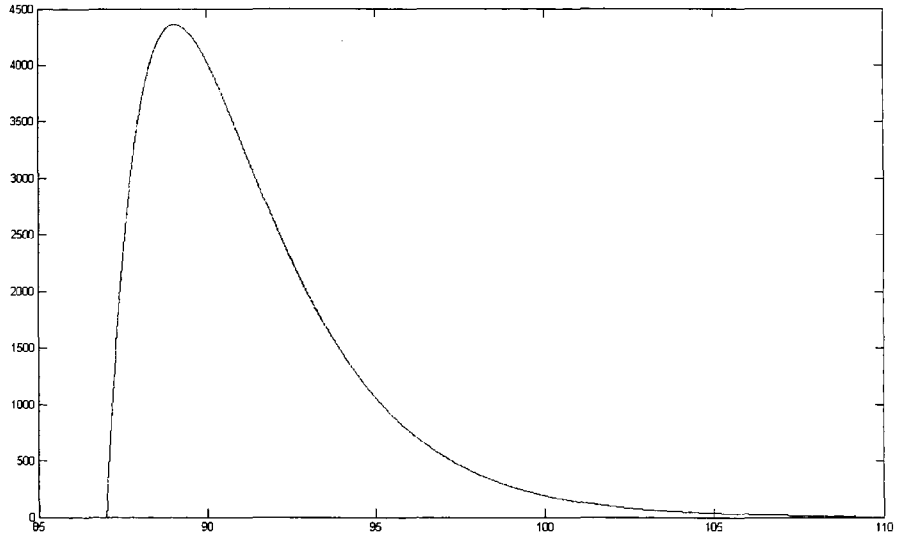

Figure 4.4, Pearson Type VI curve generated from simulated data.

4.3 Leaky-Integrate and Fire Model with Colored Noise

So far we have discussed the effect of white noise on ISI distribution. A problem of interest is to examine the effect of colored noise on neuronal dynamics. The colored noise is characterized by noise having finite correlation time. Inclusion of such a noise renders the membrane potential non-markovian (Gardiner [16]). The SDE's which characterized the system are:

$$\dot{V} = -\frac{V}{\tau} + \mu dt + \sigma_V R(t) dt \qquad (7)$$

$$\dot{R} = -\vartheta R + \sigma_R dW(t)$$

$$\langle R(t_1) R(t_2) \rangle = \sigma_R^2 e^{-\vartheta(t_2 - t_1)}$$

The colored noise can be generated from Ornstein-Uhlenbeck process. Accordingly, the colored noise R(t) in eq(7) is assumed to be governed by SDE for Ornstein-Uhlenbeck process [16]. The system of equation is given by eq(7). We employ Euler-discretization method for simulation of FPT.

$$V((n+1)h) = \left(1 - \frac{h}{\tau}\right) X(nh) + \mu h + \sigma_V R(t) \qquad (8)$$

$$R((n+1)h) = (1 - \vartheta h) R(nh) + \sigma_R \sqrt{h} Z$$

where Z0, Z1, ... are independent, identically distributed standard normal variates.

We generate standard normal variates and solve the coupled system of equations (8) for each time step. Again we use another random number and update V(t) and R(t).

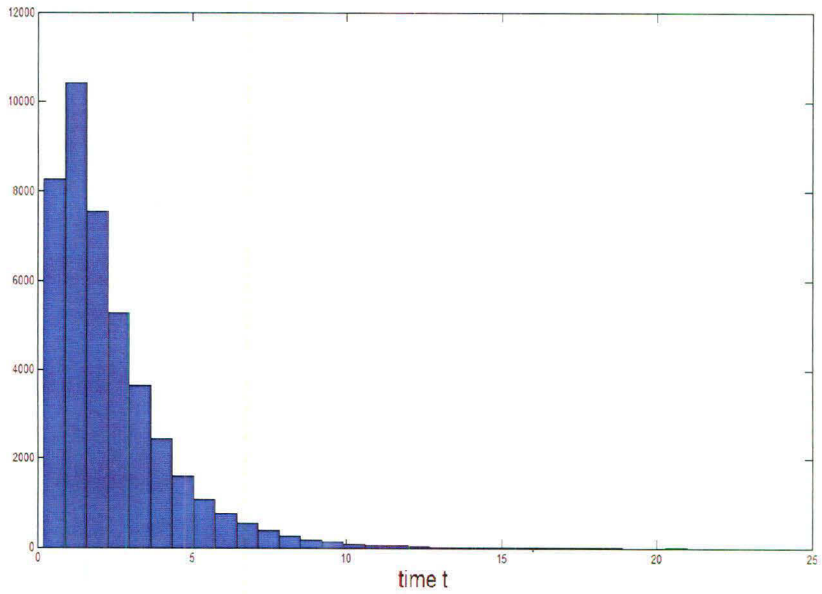

Figure 4.5a

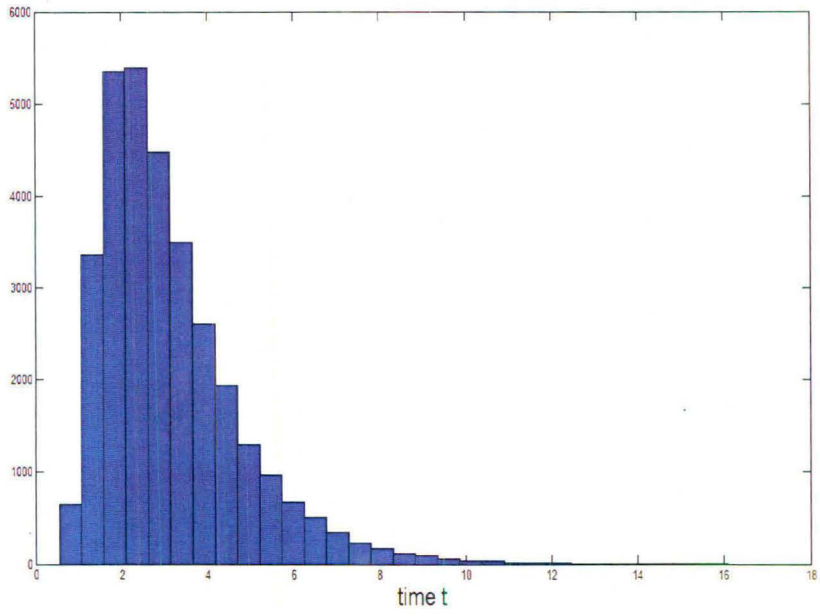

Figure 4.5b

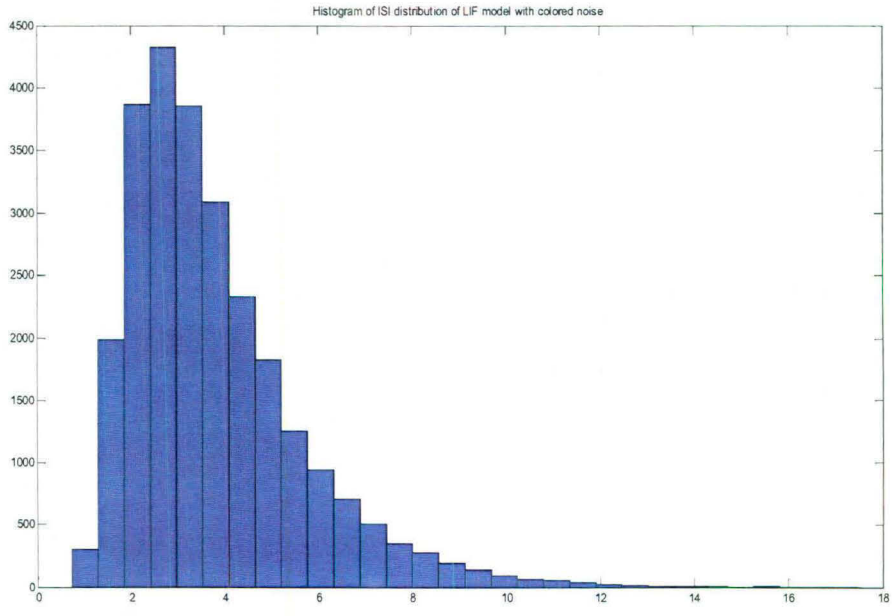

Figure 4.5c,

Figure 4.5a, 4.5b, 4.5c frequency distribution of FPT distribution with colored noise (v= 10, 50, 100)

The effect of colored noise for varying ν is exhibited in fig 6. With increasing ν, the shape of density function is becoming less-skewed.

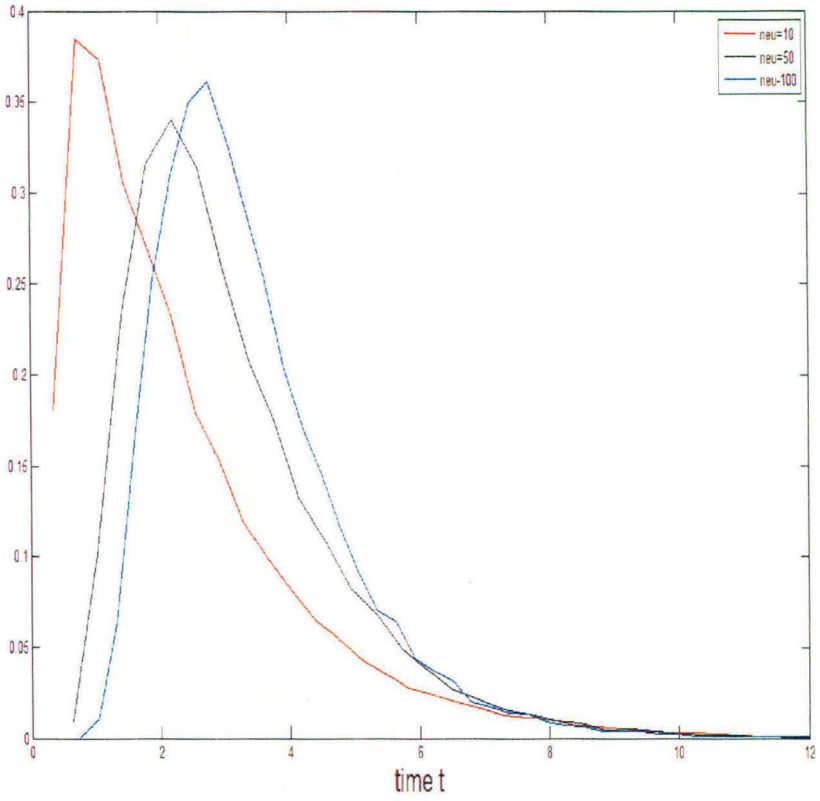

Figure 4.6, PDF of simulated ISI distribution of LIF model with colored noise at different value of neu parameter

4.4 Approximating FPT distribution by Pearson Curve

We present table the data from histogram in fig 4.5c when ν=100. Using similar analysis as done in chapter 3, we find κ=10.3804 this again points to Type VI Pearson curve.

Table 4.2: centre value of bins and frequency obtained from histogram for v=100(see fig 4.5c).

centre value of bins	frequency	First Sum	Second Sum	Third Sum	Fourth Sum
1.0192	299	26333	157378	700622	2791234
1.5775	1988	26034	131045	543244	2090612
2.1358	3866	24046	105011	412199	1547368
2.6942	4326	20180	80965	307188	1135169
3.2525	3855	15854	60785	226223	827981
3.8108	3090	11999	44931	165438	601758
4.3692	2336	8909	32932	120507	436320
4.9275	1832	6573	24023	87575	315813
5.4858	1259	4741	17450	63552	228238
6.0442	946	3482	12709	46102	164686
6.6025	703	2536	9227	33393	118584
7.1608	506	1833	6691	24166	85191
7.7192	345	1327	4858	17475	61025
8.2775	280	982	3531	12617	43550
8.8358	196	702	2549	9086	30933
9.3942	141	506	1847	6537	21847
9.9525	98	365	1341	4690	15310
10.5108	68	267	976	3349	10620
11.0692	54	199	709	2373	7271
11.6275	43	145	510	1664	4898
12.1858	27	102	365	1154	3234
12.7442	19	75	263	789	2080
13.3025	12	56	188	526	1291
13.8608	12	44	132	338	765
14.4192	11	32	88	206	427
14.9775	2	21	56	118	221
15.5358	11	19	35	62	103
16.0942	3	8	16	27	41
16.6525	2	5	8	11	14
17.2108	3	3	3	3	3

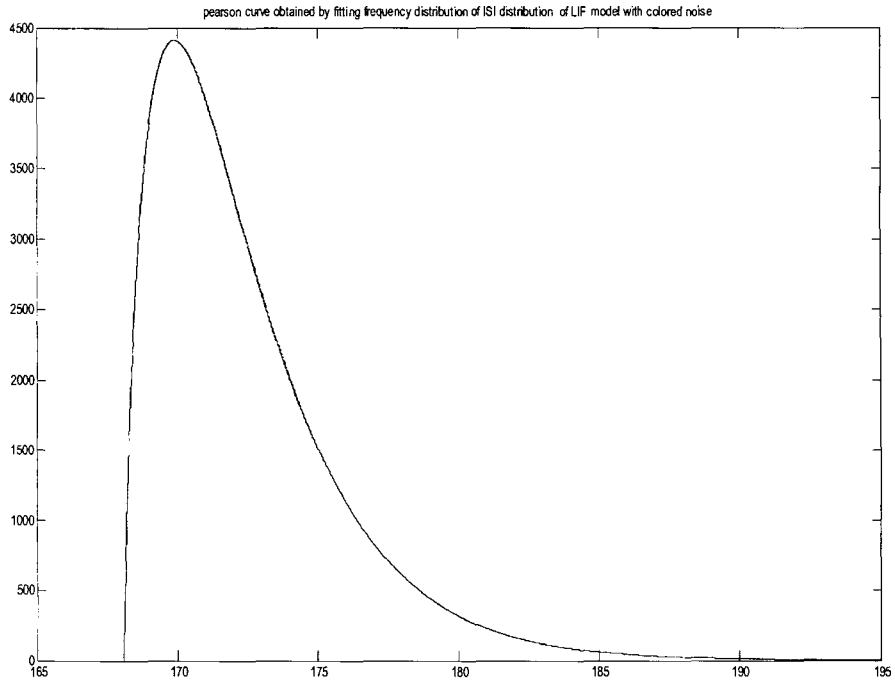

Figure 4.7, Type VI frequency distribution

4.5 Effect of ν on K L measure

The colored noise tends to white noise as $\nu \to \infty$, $\sigma^2 \to \infty$ such that $\frac{neu}{2\sigma^2} = 1$ (Gardiner [16]). It would be useful to study the effect of varying ν on FPT distribution. A quantitative measure based on K L measure can provide distance of FPT distribution from that of inverse–gaussian distribution which holds for $\nu \to \infty$. Accordingly, it is expected that D(FPT-CN||IGD-WN) will decline with increasing ν we shown in fig 4.8, the variation of K L measure with respect to ν and find as ν becomes larger and larger, K L measure becomes smaller and smaller [23].

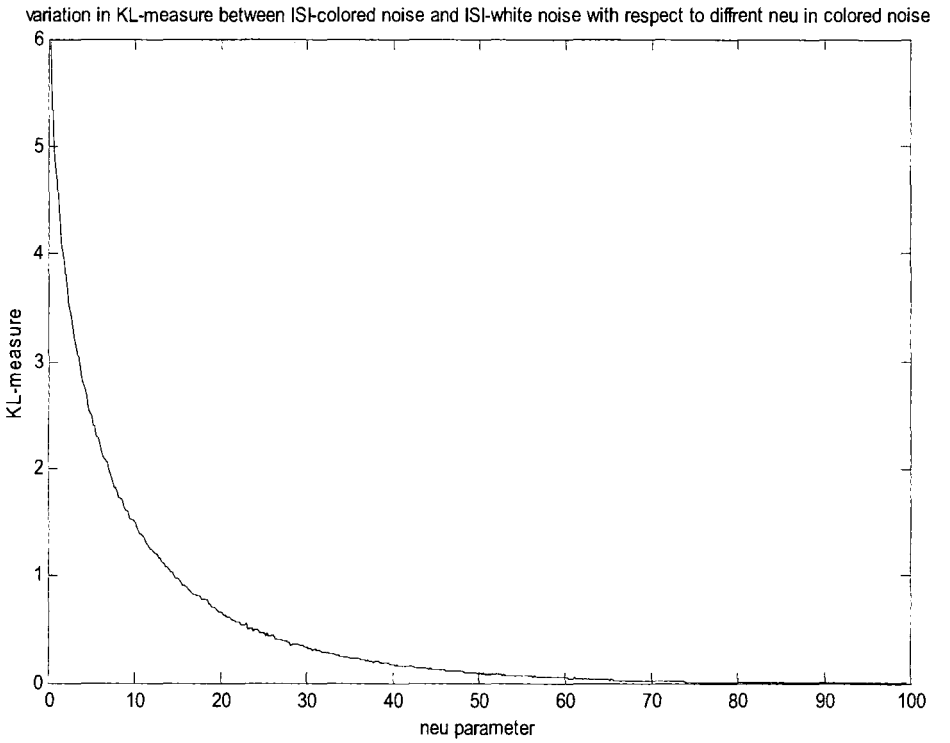

Figure 4.8, Variation of K L-measure between ISI distributions with color noise and ISI distribution with white noise.

The framework we have discussed is quite general and can be extended for other type of neuronal models with colored noise.

Chapter-5

Conclusion and Future Work

We find that ISI distribution can explicitly be obtained in a simple non-leaky integrate fire model. As neuronal models become more complicated, one has to deal with linear and nonlinear models describes by stochastic differential equations. Further, if the noise sources are colored, the analysis requires the state-space to be increased as illustrated for the case of LIF model with colored noise. The approach advanced in the dissertation is based on Monte-Carlo technique for study of SDE. The simulation study has enabled us to obtain First Passage Time of inter-spike distribution. Another contribution is to employ Pearson family of frequency curves to characterize the FPT distribution for different noise sources: we find that in all cases considered in the dissertation, type VI Pearson curve characterizes the data set. This aspect needs to bo further investigated for other types of neuronal models.

REFRENCES

1. Koch C: "Biophysics of computation". Oxford University Press.1999

2. Dayan P and Abbott L.F: Theoretical Neuroscience "Computational and Mathematical Modeling of neural system". MIT Press, 2001.

3. Gerstner W, Kistler W M: Spiking Neuron Models: Single Neurons, Populations, Plasticity: Cambridge University Press, 2001.

4. Shadlen M.N and Newsome W.T: "Noise, Neural Codes and Cortical Organization, Current Opinion in Neurobiology, vol-4, 1994, pp.569-579.

5. Robinson H.P.C: The Biophysical Basis of Firing variability in Cortical Neurons, from Computational Neuroscience: A Comprehensive Approach, Ed. Feng .J, CRC Press , 2004.

6. Tuckwell H.C and Feng J: A Theoretical Overview", from "Computational Neuroscience, A Comprehensive Approach Ed: Feng .J, CRC Press LLC, 2004.

7. Gerstein G, Mandelbrot B.L: Random Walk Models for the Spike Activity of a Single Neuron, Biophysical Journal vol 4: pp. 41-68(1964).

8. Gabbiani C and Koch .C: Principles of Spike Train Analysis in Methods in Neural Modeling: From Ions to Network, Ed: Koch .C and Segev .I, MIT Press, 1998.

9. Kapur J.N, and Kesavan H.K: Entropy optimization principle with Application, Academic Press, 1992.

10. Karmeshu (Ed): Entropy measures, maximum entropy principle and emerging applications, Springer-Verlaj 2003.

References

11. van der Lubbe .J.C.A: Information theory, Cambridge University Press 1997.

12. Moss F and Gielen S (Ed): Neuro-Informatics and Neural Modelling, Elsevier, 2001.

13. Meunier C and Segev I: Neurons as Physical objects: Structure, dynamics and function, Neuro-Informatics and Neural Modelling, Ed: Moss F and Gielen S, Elsevier, 2001.

14. Strong S.P, Koberle R, van Steveninck R.R.R and Bialek W: Entropy and Information in Neural Spike Trains: Phy. Rev. letter, vol- 80, no. 1, 1998.

15. Maio V. Di, Lansky and P, Rodriguez. R: Different Types of Noise in Leaky Integrate and fire model of Neuronal Dynamics with Discrete Periodical Input, Gen. Physiol. Biophys, vol-23, pp. 21-38, 2004

16. Gardiner C.W (Ed): Handbook of Stochastic Methods for Physics, Chemistry and the Natural Sciences, Springer, 2003.

17. Elderton W.P and Johnson N.L: Systems of Frequency Curves, Cambridge University Press, 1969.

18. Lansky. P, Ditlevsen. S: Estimation of the input parameters in the Ornstein-Uhlenbeck neuronal model, Phys Rev E 71, 011907, 2005

19. Lansky. P, Sanda. P and He. J: The parameters of the stochastic leaky integrate and fire neuronal model, J.Comput Neurosci 21:211-233, 2006

References

20. Burkitt. A.N and Clark. G.M: Calculation of Interspike Intervals for Integrate and Fire Neurons with Poisson distribution of Synaptic input" Neural Computation 12, 2000, pp. 1789-1820.

21. Kwan R and Leung C: An Accurate Method for Approximating Probability Distributions in Wireless Communication: IEEE, WCNC Proceedings 2006

22. Patil. K and Karmeshu: Effects of Randomness in Synaptic Strength on Bimodality in Sensory Neuron (submitted)

23. Lansky .P and Kostal L: "Similarity of Interspike Interval distribution and information gain in a stationary neuronal firing" Biol Cybern 94, pp. 157-167, 2006.